International Journal of Engineering and Advanced Technology (IJEAT)
ISSN: 2249-8958 (Online), Volume-7 Issue-4, April 2018

A Multilevel Inverter fed Direct Torque Control Strategy for an Induction Motor using PI Controllers

Vinod B. R., Shiny G.

Abstract: ***This paper presents a multilevel inverter fed direct torque control scheme for an open-end winding configured induction motor drive. Unlike the hysteresis controller based direct torque control strategy, the control scheme comprising of the torque and flux control by rotating reference frame quadrature-axis and direct-axis voltage components respectively. Here, Proportional Integral controllers are used for the generation of these voltage components. In the modulation part, a fractal based space vector direct torque control algorithm is used for sector identification and determination of associated switching vectors. Moreover, the algorithm incorporates a computationally efficient 60^0 coordinate system for representing the space vectors instead of the conventional Cartesian coordinate system. The speed reversal, steady-state and dynamic performance of the scheme is thoroughly analyzed under loading conditions. The multilevel inverter drive is implemented on an open-end winding type induction motor. A six level inverter fed direct torque controlled drive was designed and implemented by using a 2 Hp induction motor. The loading performance of the scheme is tested on a mechanical load with a 5Hp induction motor. All the experimental waveforms were captured under closed loop mode and the results are presented to validate the scheme.***

Index Terms: Direct Torque Control; Induction Motor; Loading; Six Level Inverter; Space Vector.

I. INTRODUCTION

Now a day, with the advanced development in the area of power electronics, processors, and control algorithms, it is possible to achieve competent control performance with AC motor drives compared with that of DC motor drives. Researchers have developed variety of control algorithms for AC motor drives to achieve precise speed/torque control of the motor in spite of the parameter variations or any other external disturbances. Among many other techniques, field oriented control (FOC) and direct torque control (DTC) have gained wide acceptability for the control of adjustable speed AC drives [1]-[4]. Compared to FOC scheme, the conventional DTC has gained popularity mainly because of its simple structure, fast control of torque and speed, and its suitability to use with multilevel inverter fed drives. DTC also ensures independent control of electromagnetic torque and stator flux without the need of complex transformations.

Manuscript published on 30 April 2018.
***** Correspondence Author (s)
Vinod B. R.*, Department of Electronics and Communication Engineering, College of Engineering Trivandrum, Thiruvananthapuram, (Kerala), India. E-mail: vinodbrcet@gmail.com
Shiny G., Department of Electronics and Communication Engineering, College of Engineering Trivandrum, Thiruvananthapuram (Kerala), India. E-mail: drgshiny@gmail.com

In spite of all its advantages, the conventional DTC technique suffer some drawbacks, such as high torque ripples that directly cause motor current distortion and variable switching frequency problem, which may lead to reduced system efficiency. The conventional DTC techniques are based on hysteresis controller for the generation of torque/flux components and look-up table approaches are used for the selection of switching voltage vectors. The hysteresis band of the controller mainly determines the output harmonic content and the look-up table based voltage selection approach becomes inefficient for the implementation of multilevel inverter fed DTC drives. Several modifications are made in the conventional DTC structure to achieve constant switching frequency operation and reduce the output ripples considerably [5]-[13].

Initially, DTC technique was introduced for voltage fed pulse width modulation (PWM) inverter drives. The increased number of switching voltage vectors, as present in the multilevel inverters can significantly reduce the output ripples to a greater extend [14]-[16]. In recent years, many research studies have been reported for the implementation of multilevel inverter with different topologies. Among these, open-end winding (OEW) configured induction motor drives are proved to be an effective topology for the realization of multilevel inverters (MLIs) [17]-[18]. Also, an attempt to implement OEW configured induction motor with DTC technique is suggested to improve the output torque ripples [19]-[20]. Moreover, research studies based on different voltage source inverter topologies are reported to eliminate the unwanted effects such as neutral-point fluctuations, isolated DC source requirement, current harmonic reduction etc., which are inherently present in a conventional DTC drive. The control algorithm based on space vector modulation (SVM) guarantees constant switching frequency operations of MLIs [21]-[26]. The adaption of SVM with multilevel inverter fed DTC drive will ensure constant switching frequency operation, which significantly suppress the output ripples to a greater extend [27]-[30].

In order to achieve reduced output ripples and constant switching frequency operation, this paper proposes SVM based DTC scheme for a multilevel inverter fed drive. Here, a generalized SVM algorithm is proposed, which ensures the freedom of section of voltage vectors offered by the multilevel inverter. The SVM algorithm utilizes a fractal theory approach for sector identification and associated switching vector generation. Also, in order to reduce the computation complexity involved in the multilevel SVM scheme, the algorithm uses a 60 *degree* coordinate system instead of the standard Cartesian coordinate system.

In the proposed method, the conventional hysteresis controllers and switching vector table modules are replaced with two proportional integral (PI) controllers, an estimator and a space vector modulator. For experimental verification of the scheme, a six level inverter fed DTC drive was designed and implemented. The drive performances were investigated under steady state, transient state and speed reversal conditions. Moreover, experimental analysis were carried out to show the effectiveness of drive in reducing the output ripples, improved current quality in terms of THD, frequency spectrum analysis and adaptability in switching to different DTC drive configurations. All the experimental results were tested under no-load and loaded conditions in closed loop for different operating modes.

II. PHYSICAL MODELING AND CONFIGURATION

A. Model of Inverter fed Induction Motor with Open-End Windings

The power circuit model proposed for realizing multilevel inversion is shown in Fig. 1 [17]. The circuit configuration consists of a six level inverter and an induction motor with open-end windings. The open-end winding induction motors are obtained by removing the neutral point of the stator windings of ordinary three phase motors. A six level inverter drive is realized by feeding a three level inverter (constituted by cascading two level inverters) at one end, and with a two level inverter at the other end. Here, each inverter is powered by an isolated DC link with asymmetric voltages. This configuration eliminates the neutral point fluctuations as isolated DC power supplies are employed to power the individual inverters. Inverter-1, inverter-2, and inverter-3 are fed with a dc voltage of $2V_{dc}/5$, $2V_{dc}/5$, and $V_{dc}/5$ respectively, where V_{dc} is the dc voltage applied to a conventional two level inverter drive system. As shown in Fig. 1, the points O and O' are not connected each other so that there is no zero-sequence currents (currents of the triplen harmonic order) flow through the motor phases. Thus the entire triplen harmonic content in the motor phase voltage is dropped across the points O and O'. The proposed topology is capable of attaining one of the six possible voltage level values: $-V_{dc}/5$, 0, $V_{dc}/5$, $2V_{dc}/5$, $3V_{dc}/5$ and $4V_{dc}/5$ across three phases of the motor, assuming that the points O and O' are short circuited. Table I illustrates the status of top switches (S_{11}, S_{21}, S_{31}) to attain six different voltage levels. The pole voltage of any phase of inverter-A (for example V_{R2O}, Fig. 1) can attain voltages of 0, $2V_{dc}/5$, $4V_{dc}/5$ by turning on top switch or bottom switch. Similarly, inverter-B can attain two different voltage level values: 0 and $V_{dc}/5$. It may be noted that the pole voltage of a given phase in inverter-A and Inverter-B ($V_{R3O'}$, in Fig. 1) attains zero voltage, if the bottom switch of the corresponding inverter is turned *ON*. However, three switches (S_{24}, S_{26}, S_{22}) are to be rated to block a voltage of $4V_{dc}/5$ and for inverter-3, it is only $V_{dc}/5$. The phase voltage across each winding of the motor under OEW configuration is obtained by

$$V_{R1R2} = V_{R1O} - V_{R2O'}$$
$$V_{Y1Y2} = V_{Y1O} - V_{Y2O'}$$
$$V_{B1B2} = V_{B1O} - V_{B2O'} \quad (1)$$

TABLE I. REALIZATION OF VOLTAGE LEVELS (*R*-PHASE) FOR SIX LEVEL INVERTER

INV-1 (S_{11})	INV-2 (S_{21})	INV-3 (S_{31})	INV A (V_{R2O})	INV B ($V_{R3O'}$)	Motor phase voltage ($V_{R2R3} = V_{R2O} - V_{R3O'}$)	Levels
OFF	OFF	ON	0	$V_{dc}/5$	$-V_{dc}/5$	0
OFF	OFF	OFF	0	0	0	1
OFF	ON	ON	$2V_{dc}/5$	$V_{dc}/5$	$V_{dc}/5$	2
OFF	ON	OFF	$2V_{dc}/5$	0	$2V_{dc}/5$	3
ON	ON	ON	$4V_{dc}/5$	$V_{dc}/5$	$3V_{dc}/5$	4
ON	ON	OFF	$4V_{dc}/5$	0	$4V_{dc}/5$	5

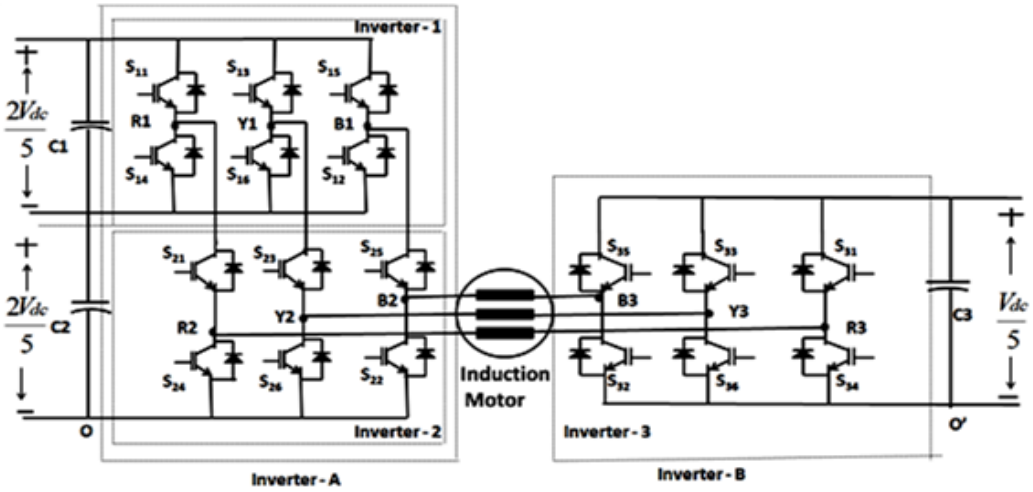

Fig. 1 Power Circuit of a six Level Inverter Drive System

Published By:
Blue Eyes Intelligence Engineering
and Sciences Publication (BEIESP)

III. PROPOSED SIX-LEVEL INVERTER FED DTC BASED ON SPACE VECTOR MODULATION

A. Principle of Direct Torque Control of an Induction Motor

The principle of DTC is based on independent control of torque and flux components, which provides a fast and vigorous response with simple structure. The primary objective of DTC is to control the electromagnetic torque and the magnitude of the stator flux linkages independently. In DTC scheme, when an induction motor is fed from a voltage source inverter, it is required to find the output stator voltage vector components along rotating $d-q$ axis and stationary $\alpha-\beta$ axis. The output stator voltage vector equation with the stator resistance drop neglected can be written as

$$V_s = \frac{\mathrm{d}\emptyset_s}{\mathrm{dt}} \tag{2}$$

Thus, the output voltage vector for time duration of Δt, the change in the stator flux vector is

$$\Delta\emptyset_s = V_s * \Delta t \tag{3}$$

Therefore, for each applied inverter voltage vector, the stator flux vector changes by a small amount along the direction of applied voltage vector. This will cause a change in slip speed, which in turn will change the torque parameter. The electromagnetic torque equation for an induction motor is defined as

$$T_e = \frac{3}{2}\left(\frac{P}{2}\right)\frac{L_m}{L_r L'_s}(\emptyset_r \text{ X } \emptyset_s) \tag{4}$$

where $L'_s = L_s L_r - {L_m}^2$ is the total stator inductance, L_m is the magnetizing inductance, L_s is the stator inductance, L_r is the rotor inductance, $\emptyset_s$ and $\emptyset_r$ are the stator and rotor flux vectors, and P is the number of poles.

The torque equation can be modified as

$$T_e = \frac{3}{2}\left(\frac{P}{2}\right)\frac{L_m}{L_r L'_s}(|\emptyset_r| \, |\emptyset_s| \sin\theta) \tag{5}$$

where, θ is the angle between the stator and rotor flux vectors.

In conventional DTC, the trajectory of stator flux depends on the selection of inverter active voltage vectors. Fig. 2 shows the voltage vector selection of a conventional two level inverter with six active vectors V_1, V_2, V_3, V_4, V_5 and V_6. The selection of active voltage vectors will result in the change of slip speed, which in turn will affect both the torque component (τ_e in Fig. 2) and flux vector component (ϕ_s) simultaneously. For the condition shown in Fig. 2, it is to be noted that for any one of the active vectors from among V_2, V_3, V_4 will cause an increase in the stator flux angle from its present position. Hence the torque increases due to an increase in slip speed. Furthermore, the stator flux angle can be decreased by the selection of V_1, V_5 and V_6 voltage vectors. Now the torque reduces due to a decrease in slip speed. It is observed from Fig. 2 that the selection of active voltage vectors positioned in between angles 90^0 to 270^0 with respect to the α-axis will result in the reduction of stator flux magnitude irrespective of stator voltage vector position. Also at zero vector (V_0 or V_7) condition, the flux and torque are unaltered. Thus, the magnitude and direction of flux and torque vector components depends on the applied active voltage vectors.

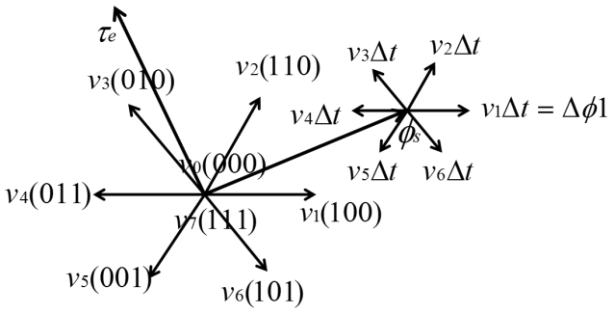

Fig. 2.Switching vector selection in a 2-level inverter fed DTC

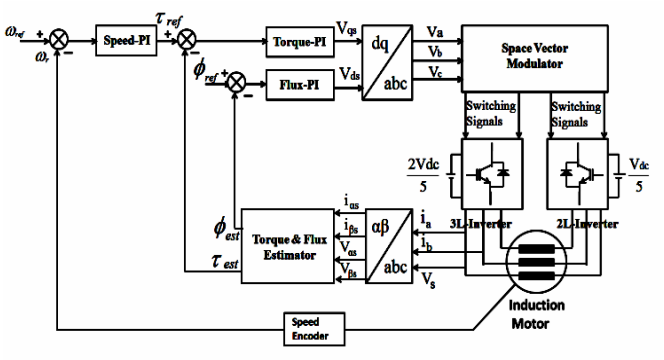

Fig. 3.Block diagram of 6L-MLI DTC with OEW IM

B. Switching Strategy of the Proposed PI Controller based DTC for an Induction Motor

The presence of hysteresis controllers in any drive will cause variable switching frequency problem and unpredictable output torque ripples. In the proposed DTC scheme (Fig. 3), the conventional hysteresis controllers are replaced with effective PI controllers for generating the torque and flux control parameters. In the proposed method, the torque control is achieved only by controlling the rotating frame quadrature-axis voltage component, V_{qs} and the flux control is achieved by controlling the direct-axis voltage component, V_{ds} in the rotor-reference frame. These control parameters (V_{ds}, V_{qs}) are generated based on the torque error and flux error. As shown in Fig. 3, these errors are generated by comparing the respective reference and estimated parameters and the errors are processed by the flux and torque PI controllers.

A J260 shaft encoder is used to measure the rotor speed. The output of the encoder is converted into a speed signal by using a frequency to voltage converter. The speed control loop generates the torque reference through the PI controller. The control loop will generate the speed error, based on the comparison of actual shaft speed sensed with an encoder and the speed command signal. The flux reference is given directly to a flux PI controller, which should ensure the motor to operate in constant flux region. In this scheme, the torque,

Published By:
Blue Eyes Intelligence Engineering
and Sciences Publication (BEIESP)

stator flux and axis angle θ_{est} values are estimated using stator currents, voltage and torque equation of an induction motor model. The stator current and voltage values are measured from inverter output terminals. The torque and flux values are estimated using the sensed stator voltage and stator currents. Here, stationary frame parameters are used for all the calculations and stator resistance is the only motor parameter used for all estimations. The basic equation for the estimation of stator flux is given as

$$\emptyset_s = \int (V_s - i_s R_s) dt \quad (6)$$

where V_s, i_s and R_s are the stator voltage, current and coil resistance of the motor. Here, motor resistance drop is also considered for flux estimation.

The stator flux phasor is given by

$$\emptyset_s = \emptyset_{\alpha s} - j\emptyset_{\beta s} \quad (7)$$

Therefore, the magnitude of the estimated stator flux is

$$|\emptyset_{est}| = \sqrt{\emptyset_{\alpha s}{}^2 + \emptyset_{\beta s}{}^2} \quad (8)$$

Now, the stator flux components along the $\alpha - \beta$ axes can be calculated as

$$\emptyset_{\alpha s} = \int (V_{\alpha s} - i_{\alpha s} R_s) dt \quad (9)$$

$$\emptyset_{\beta s} = \int (V_{\beta s} - i_{\beta s} R_s) dt \quad (10)$$

Similarly, the estimated motor torque is estimated by

$$T_{est} = \frac{3}{2} P(\emptyset_{\alpha s} i_{\beta s} - \emptyset_{\beta s} i_{\alpha s}) \quad (11)$$

Fig. 4 shows the torque and flux regulators used for generating the flux vector component V_{ds} and the torque component V_{qs}. The torque-flux regulator used in the present study consists of PI controller along with saturation block. Here, speed, torque and flux PI controllers are tuned to measure proportional gain (K_p) and integral gain (K_i). The values obtained are given in Table II.

In this scheme, a torque-flux regulator is used along with SVM algorithm. The presence of PI controllers reduces large variation in torque ripples and the SVM algorithm ensures constant switching frequency operation. The tuned outputs from the proposed torque-flux PI controller will result torque component V_{qs} and flux component V_{ds} based on torque/flux errors respectively.

TABLE II. PI CONTROLLER PARAMETERS

Speed PI Controller		Torque PI Controller		Flux PI Controller	
Kp	Ki	Kp	Ki	Kp	Ki
50	3	2.2	0.5	20	0.3

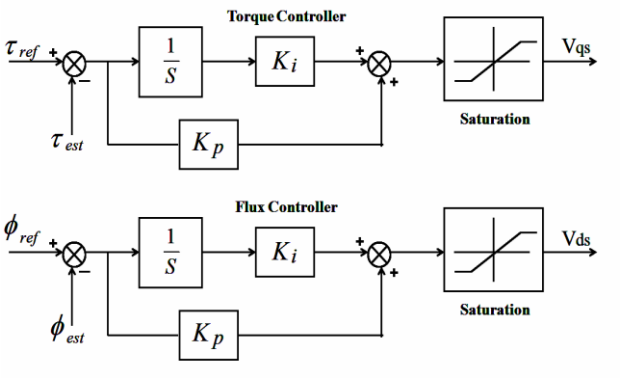

Fig. 4.PI Controller based Torque-Flux Regulators

The proposed method also has the configuration flexibility to operate in any one of the mode from 2L-DTC to 6L-DTC. The selection of operating mode is determined by the value of modulation indices. Here, the saturation block act as a limiter and its level determines the operating modulation index value.

As shown in Fig. 3, this work utilizes a space vector based modulator for the generation of PWM signals to drive the inverter. The proposed scheme make use of a six level inverter fed control, which in turn will increase the complexity in the selection of a voltage vector from among 216 switching vectors compared to 8 switching vectors in the case of conventional two level DTC scheme. The present scheme eliminates the voltage vector selection table approach, instead uses an effective fractal based algorithm for the generation of switching voltage vectors. For the generation of inverter switching signals, it is required to apply three phase voltage signals (V_a, V_b and V_c) to a modulator. In this work, a space vector based modulator is used for the design and implementation of switching signals to drive the inverters. The reference voltage vector for space vector based DTC is given by

$$V_s = V_{ds} + jV_{qs} \quad (12)$$

Where V_s is the magnitude of reference space-vector voltage and V_{ds}, V_{qs} are voltage vector components along $d - q$ subspace respectively. The suggested DTC algorithm proposes a generalized transformation technique for the generation of voltage phase signals from the flux and torque PI controller's output. From the tuned flux component V_{ds}, torque component V_{qs} and estimated angle θ_{est}, the voltage components along the stationary reference frame can be measured. Depending on the stationary frame voltage components, the three phase voltage signals V_a, V_b and V_c can be determined by simple transformations.

The DTC algorithm proposed is independent of the type of space vector modulator used. Hence, it gives much flexibility in applying direct torque control schemes with higher level inverter drives. Moreover, overall control performance of the scheme can be simplified by the introduction of PI controllers, which in turn will generate rotating reference frame voltage components.

Published By:
Blue Eyes Intelligence Engineering and Sciences Publication (BEIESP)

IV. MODULATION STRATEGY FOR THE PROPOSED DRIVE

A. Fractal based Modulation Scheme for the Proposed Inverter Drive

The main cause of having high output ripples in the conventional DTC drives are mainly due to the limited number of voltage vectors available for switching. For example, for a two level DTC drive only 6 active vectors are available for switching. In higher level DTC drives more switching vectors are available. In the proposed six level DTC scheme, a total of 216 switching vectors are present. The increase in the number of switching vectors for the implementation of SVPWM will cause a reduction in output ripples as well as the total harmonic distortion (THD) to a greater extend. This paper proposes a SVPWM algorithm based on fractal theory. The fractal based SVPWM algorithm is proved to be an efficient algorithm for multilevel inverter drives [22]-[24].

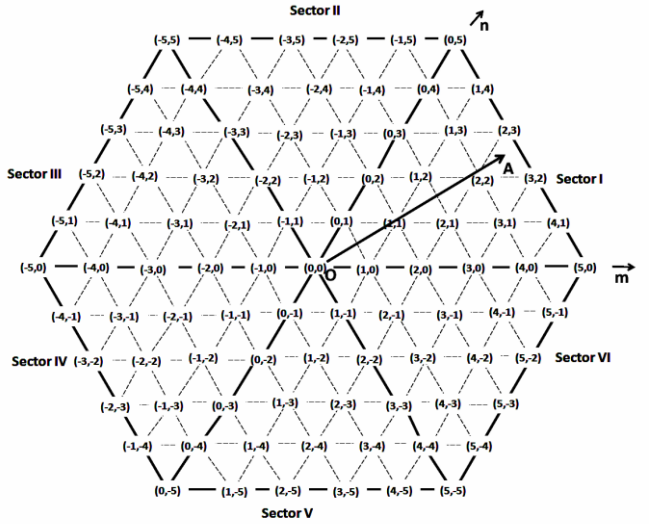

Fig. 5.Six-Level Space Vector Diagram

The space vector (SV) diagram of a six level inverter is shown in Fig. 5. It can be seen that the space vector diagram of a six level inverter consists of 150 small sectors with a total of 216 switching vectors. These switching vectors are placed in 91 switching locations. In order to reduce the computational complexity, the space vector locations are represented in a 60 *degree* $m-n$ coordinate system [21]. It can be seen from Fig. 5 that all the switching vector locations are represented as integer coordinate values.

B. Switching Vector Generation for Six Level Inverter Structure

The procedures used for implementing the fractal based SVPWM scheme are described in [22]-[24]. As the number of levels of inverter increases, the sector identification becomes a tedious process. In this work, an effective triangularisation algorithm based on fractal geometry concept is used for sector identification. For even level inverter configurations, it is not possible to apply the triangularisation process directly. However, by making proper modifications in the fractal algorithm, it can be used for sector identification of even level inverters [23]-[24].

For any n level inverter, each switching vector will be normalized through $V_{dc}/(n\text{-}1)$ factor. The space vector diagram of a six level inverter can be observed to be organized into five layers, each having a width of $V_{dc}/5$. The fractal concept cannot be directly applied to an even level inverter. To apply the fractal algorithm, SV diagram of the proposed six level inverter is transformed into the nearest SV representation in which the fractal algorithm can be directly applied. From Fig. 6, it is observed that nine level SV diagram can be achieved by adding three layers (each having a width of $V_{dc}/5$) to the existing six level SV diagram. Now, the end active vector (8 0 0) of nine level SV diagram will point to an apparent DC supply voltage of V^*_{dc} and is given by

$$V_{dc^*} = V_{dc} + 3V_{dc}/5 = 8V_{dc}/5 \quad (13)$$

Here, the DC supply voltage corresponding to active vector (5 0 0) still remains at V_{dc} only.

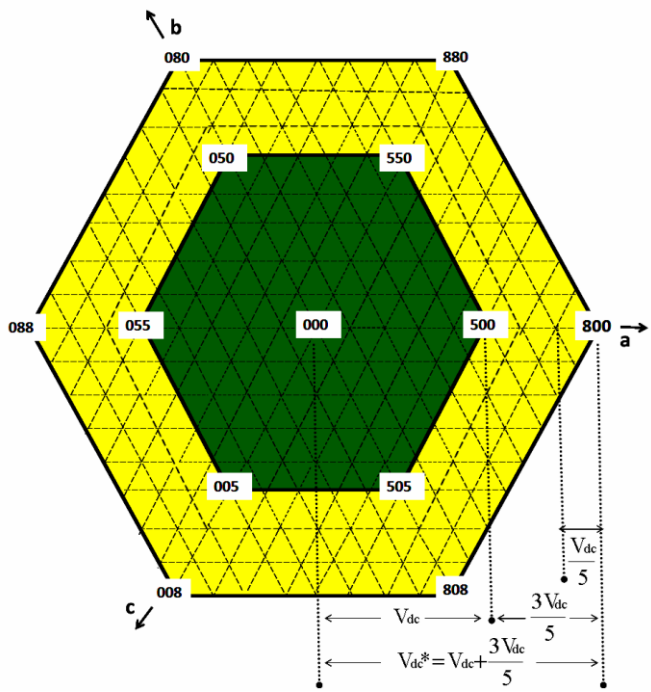

Fig. 6. Additional Three Layers To Six Level Space Vector Diagram.

Three triangularisation iterations are required for realizing a nine level SV representation. Here, after the third iteration, the original sector-I splits into a total of 64 sectors. Therefore, on considering all the sectors of the SV diagram will result a total of 384 (64x6) sectors for a nine level inverter. Even though the total number of sectors present in a six level inverter is 150, the algorithm requires three triangularisations for identifying the sector in which the tip of the reference space vector lies. After identifying the sector, a mapping and reverse mapping algorithms, as explained in [23]-[24], are used for finding out the actual switching vectors. All the dwell time calculations are done in the two level inverter modes only [26].

Published By:
Blue Eyes Intelligence Engineering
and Sciences Publication (BEIESP)

Since the switching vectors are represented in a 60 *degree* coordinate system, simple arithmetic computations are enough for calculating actual switching vectors directly [23].

V. EXPERIMENTAL RESULTS AND PERFORMANCE VALIDATIONS

For experimental validation of the scheme, the proposed PI controller based multilevel DTC algorithm is implemented on a six level inverter fed induction motor drive. The experimental set up consists 7.5KW IGBT based inverters, 2-Hp, 3-phase induction motor with open end winding structure, a mechanical loading set up and FPGA board. Here, a dSPACE module is used for the real time interface and the control strategies are implemented on a DS-1104 R&D controller board based on TMS320F240 DSP processor. The gating signals for driving the IGBT switches in the inverters are generated by a Sparton-3E FPGA board. All the experimental waveforms are captured using DPO 3034, 3Gs/s Oscilloscope. The performance of the scheme is investigated to prove qualitative improvement in terms of reduction of motor current THD and output ripples over wide speed range.

The loading performance of the scheme is verified on a strain-gauge type mechanical load with a 5 Hp induction motor. The dynamic and steady state behavior of the drive is verified under no-load conditions. Also, with the help of a loading system, experimental results were taken by operating the drive under different loaded conditions. The proposed drive can operate in two level/three level DTC mode (low speed region), four level/five level DTC mode (medium speed region) and six level DTC mode (high speed region). In this work, experimental speed tests were carried out mainly under low speed, medium speed and high speed regions.

For the proposed scheme, it is not required to switch all the three inverters at the same time. Here, only inverter-3 is switched in the lowest speed range, whereas inverter-1 and inverter-2 remains in the idle state. In the medium speed range, inverter-2 and inverter-3 are switched, while in the high speed range, all the three inverters are switched. Since inverter-1 and inverter-2 are not switched in the lowest speed range, the switching losses are entirely due to the switching of inverter-3 only. Similarly in the middle range of speed, the switching losses are due to the switching of inverter-2 and inverter-3 only. Hence it is required to switch all the three inverters only in the high speed operating region.

In addition, the speed reversing capability of the scheme is experimentally verified under closed loop mode and it is compared with the conventional DTC scheme. A 1024-pulse incremental encoder J-260 is mounted on the rotor shaft to capture the actual rotor speed of motor. The measured speed information was utilized by the speed PI controller for the generation of torque reference.

A. Steady-State and Dynamic Performance

Under steady state condition, the proposed drive is experimentally operated in a speed control mode with constant reference speed command. The prime advantage of the scheme is that it is possible to operate the drive under different DTC configurations by preserving simple DTC structure. Here, the scheme provides flexibility in switching to different inverter level DTC modes by proper configuration of PI regulators and suitable selection of modulation indices. Therefore, the steady-state performance of the scheme is investigated by subjecting the drive to operate in six level DTC, five level DTC and four level DTC modes. In all these three modes, the drive is allowed to operate under the worst no-load condition. The effectiveness of the speed control capabilities of the scheme under different DTC modes are described in the following sections.

Speed behavior during six level DTC operation: To study the performance of the drive in this mode, the experimental motor current, phase voltage and pole voltage under steady state conditions are measured and are shown in Fig. 7. It can be observed that the drive attains a maximum speed of about 1300 rpm and results least distorted motor current waveform. The drive is designed to operate in six level DTC mode by keeping a modulation index value of 0.85. It can be seen that the motor current ripples are greatly reduced in this region and the current THD value is reduced to about 4.91%. It can be seen that six level DTC mode results lowest current THD value compared to other mentioned DTC modes.

Fig.8 shows the steady state motor current and corresponding speed signal during six level DTC mode. It is observed that if the motor rotation is in clockwise direction, it give rise to a negative speed signal and vice-versa.

Speed behavior during five level DTC operation: The medium speed range steady state behavior is verified by operating the motor in five level DTC modes. Fig. 9 corresponds to experimental phase voltage, pole voltage and motor current waveforms captured during five level DTC mode. Also, it is observed from the motor current waveform that the ripples are better eliminated and results in a THD reduction of 5.67%.

Speed behavior during four level DTC operation: The drive can be configured to operate in this mode by keeping the modulation index value to 0.50. The waveforms shown in Figs. 10 represent the four level phase voltage, pole voltage and motor current captured through experimental set up. Compared to higher level DTC schemes, the current ripples obtained are more and current THD is increased to about 8.72%. Observing all the experimental results, it can be deduce that, DTC with higher level inverter configuration results lowest percentage reduction of current THD.

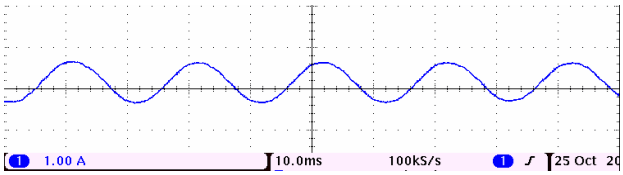

(a)

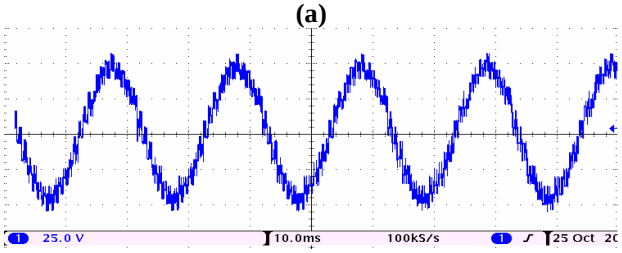

(b)

Published By:
Blue Eyes Intelligence Engineering and Sciences Publication (BEIESP)

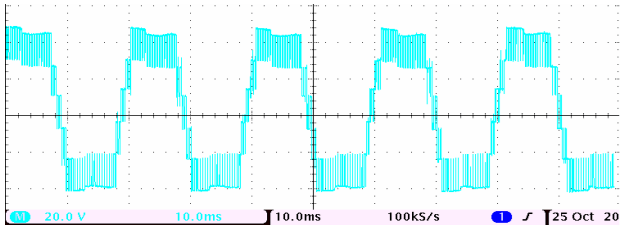

(c)

Fig. 7.Experimental Six level DTC waveforms: (a) motor current, (b) phase voltag, and (c) pole voltage.

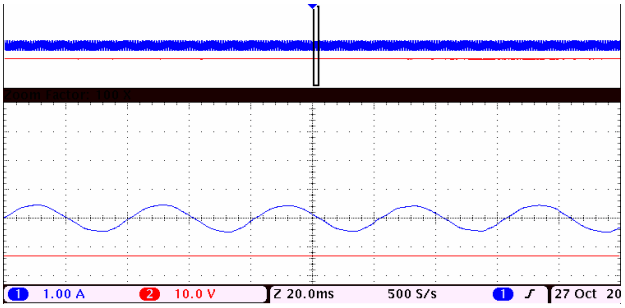

Fig. 8.Experimental Steady State Current and Speed Signal During Six Level DTC Mode.

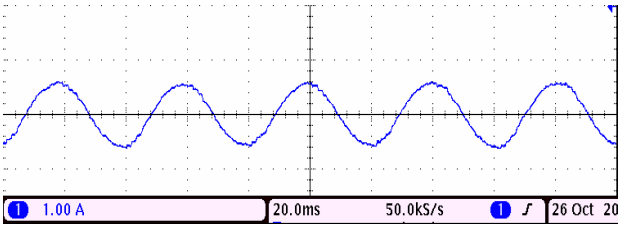

(a)

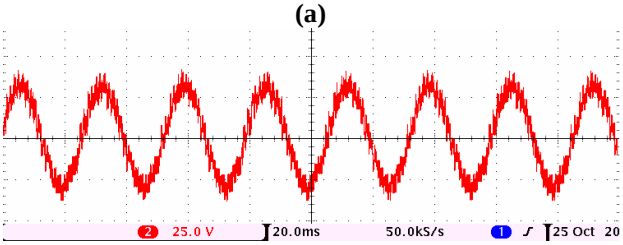

(b)

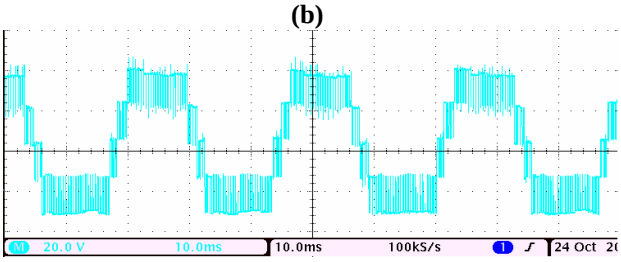

(c)

Fig. 9.Experimental Five level DTC waveforms: (a) motor current, (b) phase voltag, and (c) pole voltage.

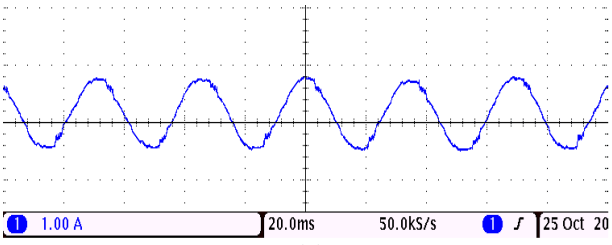

(a)

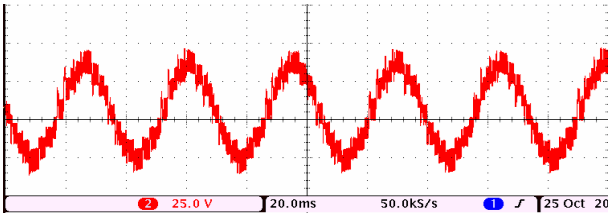

(b)

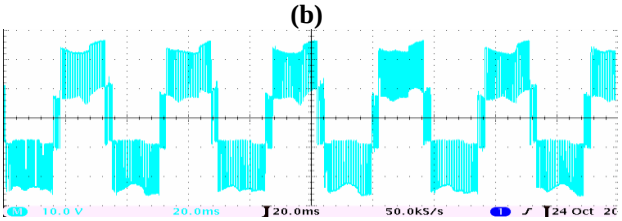

(c)

Fig. 10. Experimental four level DTC waveforms: (a) motor current, (b) phase voltag, and (c) pole voltage.

The dynamic performance of the proposed DTC drive is investigated by operating the drive from zero speed to a steady state rated speed. During transient operating region, the motor is allowed to start from rest and accelerates to attain a steady state speed. Fig. 11 shows the motor current waveform experimentally captured, when the motor starts from rest and then accelerates to attain a steady state speed of about 1300 rpm (operates from two level to six level DTC mode) under the worst no-load condition.

To evaluate the motor current quality, THD is calculated for each DTC mode under no-load condition. Table III indicates the motor current THD obtained under different DTC operating modes with designed modulation index values. It can be observed that, the motor phase current becomes smoother and the current distortions are greatly reduced for higher level inverter DTC modes. The frequency spectrum of phase voltages in each of four level, five level and six level DTC modes were captured and displayed in Fig. 12. The spectrum gives an indication of rejection of acoustic noise developed in the motor. From the spectrum it can be seen that, noise spikes are concentrated more around switching frequency of 2.5 KHz and its multiples during lower level inverter DTC modes. The spreading effect of the phase voltage spectrum is a measure of reduction of acoustic noise generated from the motor [25]. It is observed that the voltage spectrum of the proposed six level DTC scheme has better harmonic spreading property compared to a two-level inverter DTC mode.

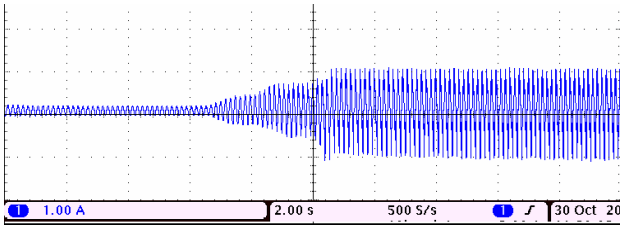

Fig. 11. Experimental Motor Phase Current During Acceleration From Two Level to Six Level DTC Modes.

Published By:
Blue Eyes Intelligence Engineering and Sciences Publication (BEIESP)

TABLE III. COMPARISON OF MOTOR PHASE CURRENT THD

Mode	2L-DTC	3L-DTC	4L-DTC	5L-DTC	6L-DTC
Modulat-ion index	0.15	0.25	0.43	0.65	0.83
THD (in %)	14.88	13.93	8.72	5.67	4.91

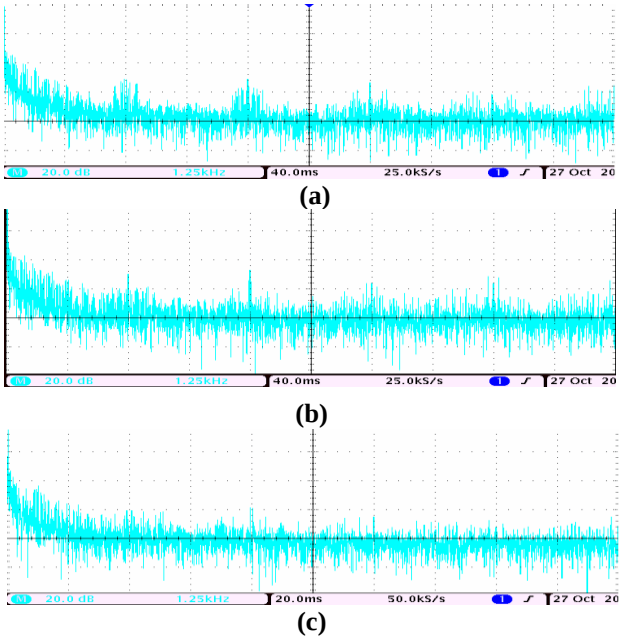

Fig. 12. Experimental Motor Current Frequency Spectrum During: (a) four level DTC, (b) five level DTC, and (c) six level DTC.

B. Performance under Speed Reversal

To study the performance of the drive for speed reversal control, the motor is allowed to rotate either in clockwise or in anti-clockwise direction under the influence of a speed reference command signal. The speed reference is given in such a way that, the motor decelerates with a constant slope, comes to stop condition, and then accelerates with a steady state speed in the opposite direction. Here, a speed variation of reference command from 1300 rpm to -1300 rpm is chosen and the experimental results obtained is given in Fig. 13(a) and also the waveform captured during the speed reversal from clockwise to anti-clockwise direction with the same speed is shown in Fig. 13(b). It can be observed that smooth transition of the motor current occurs at the time of speed reversal and also, the current magnitude varies linearly during decelerating and accelerating speed regions. In addition, Fig. 14 indicates the experimental stator flux components ($\emptyset_{\alpha s}$, $\emptyset_{\beta s}$) along $\alpha - \beta$ axis during speed reversal condition. From this figure, it is clear that initially, $\emptyset_{\alpha s}$ leads $\emptyset_{\beta s}$ and after the speed reversal, $\emptyset_{\beta s}$ leads $\emptyset_{\alpha s}$ which validates the speed reversal property and the resulting transition is also indicates to be smooth.

C. Loading Performance

Using a strain gauge type mechanical loading system with a 5 Hp induction motor, the performance of the proposed drive is tested under different loading conditions. The motor current was measured for analyzing the loading performance of the prescribed drive. In this set up, it is possible to have linear variation of load from no-load to full-load condition and vice-versa. Fig. 15(a) indicates the zoomed motor current captured experimentally, when motor load changes from no-load to full-load toque of 6 N.m. The interesting observation is that, the current magnitude linearly increases with increase in load torque. Fig. 15(b) describes the dynamic motor current response with a changed load torque from 6 N.m to 0 N.m. The interesting observation is that, the worst motor current in terms of quality, results under no-load condition and the current magnitude as well as the motor current quality improves under full-load condition. Fig. 16 shows the comparison of motor current THD against number of DTC levels. It can be observed from the comparison chart that, as the inverter level of DTC scheme increases, the motor current THD is reduced drastically. The experimental results indicate that the proposed six level DTC generates lowest THD value.

The above analyses indicate the performance improvement of the proposed six level DTC scheme, when compared with the mentioned lower level DTC schemes. The experimental sets up details of the proposed drive with the loading system are shown in Fig. 17.

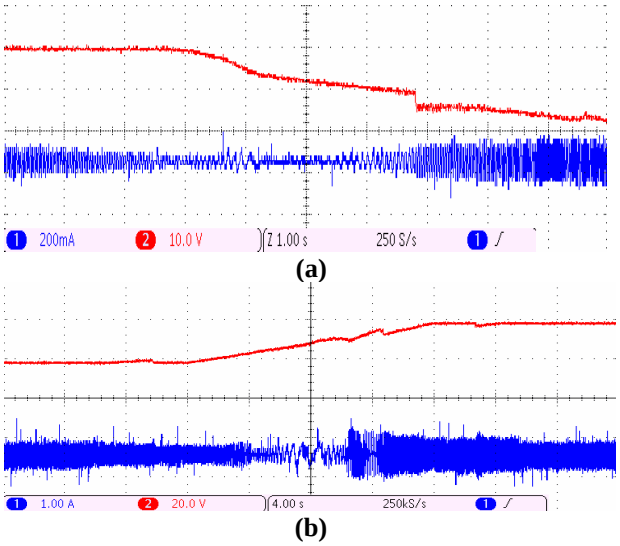

Fig. 13. Experimental speed signal and motor current during speed reversal condition: (a) speed reversal from anti-clockwise to clockwise, (b) speed reversal from clockwise to anti-clockwise directions.

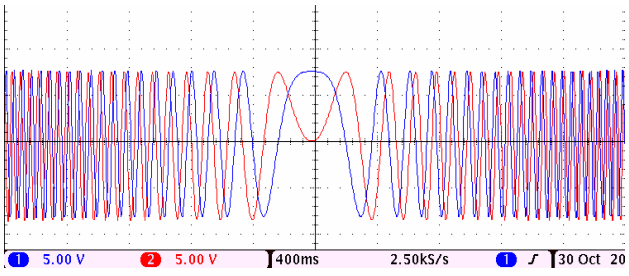

Fig. 14. Experimental Stator Flux Waveform During Speed Reversal.

Published By:
Blue Eyes Intelligence Engineering and Sciences Publication (BEIESP)

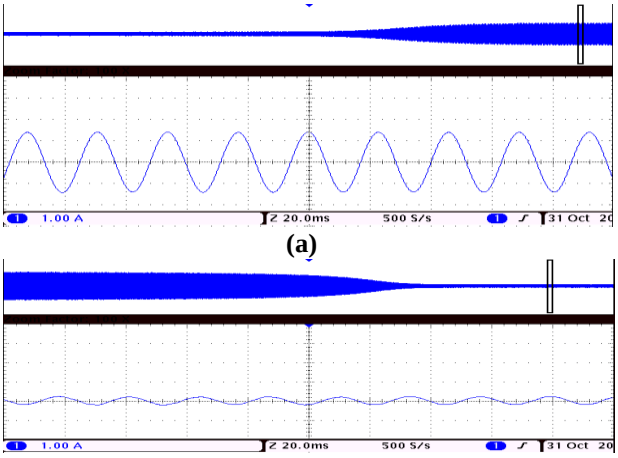

(a)

(b)

Fig. 15. Experimental during loading conditions: (a) no-load to full-load, (b) full-load to no-load.

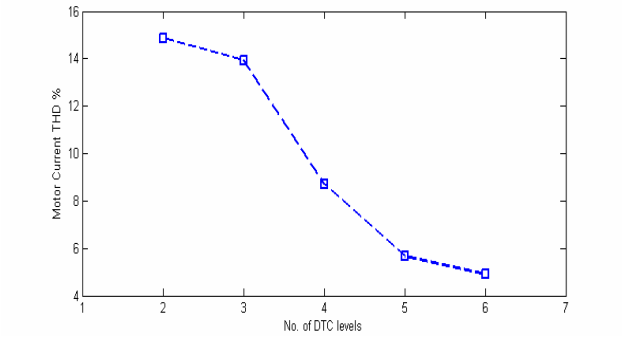

Fig. 16. THD Comparison of Motor Current at Different DTC Levels.

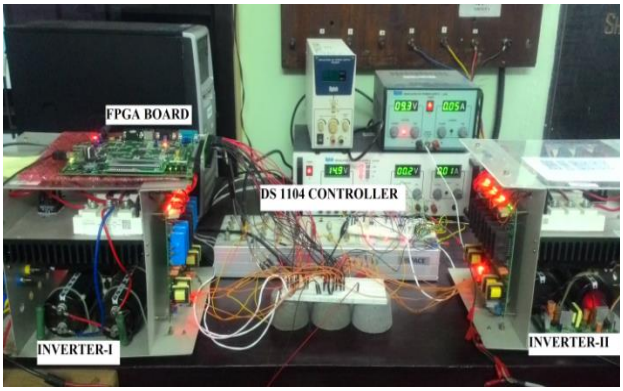

(a)

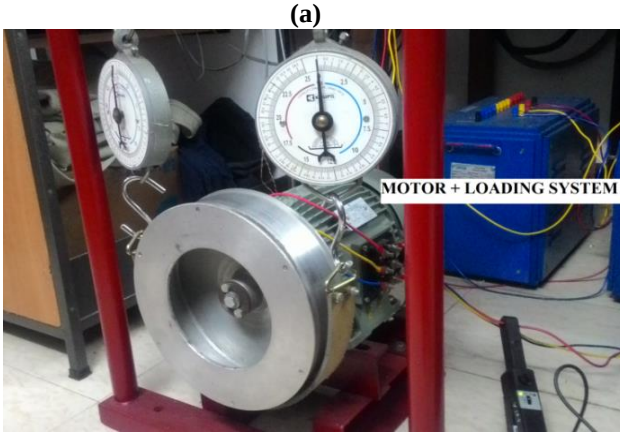

(b)

Fig. 17. (a) Experimental set up, (b) Loading system

VI. CONCLUSION

In this study, space-vector modulated DTC scheme is proposed for an open-end winding configured induction motor drive with reduction in output ripples and current THD. Here, a six level inverter fed DTC scheme is designed and implemented on a 2 Hp induction motor drive. The loading performance the proposed drive is validated through a strain-gauge type mechanical load with a 5 Hp induction motor. The gating signals to drive the power switches are generated from a FPGA controller. The major contribution in the proposed design is its effective integration of SVM technique with any *n*-level multilevel inverter fed DTC drive. A fractal based space-vector DTC algorithm is used in the proposed design, which is more suitable for MLI-DTC configurations. The performances of the scheme under transient, steady-state and speed reversal operating conditions were studied and experimental results are presented to validate the scheme. The proposed method significantly improves the motor current quality in terms of current THD and its value reduces to 4.91%, when operated in six level DTC mode. The experimental results prove that the proposed scheme can be effectively configured to operate from two level DTC mode to six level DTC mode, with the observation that the current THD performance improves for higher level DTC drives. Moreover, this proposed methodology can be easily adapted to any *n*-level inverter fed DTC controller without significant modifications.

REFERENCES

1. I. Takahashi and T. Noguchi, “A new quick-response and high efficiency control strategy of an induction motor,” IEEE Trans. on Ind. Appl., vol.IA-22, pp. 820–827, Sep. 1986.
2. D. Casadei, F. Profumo, G. Serra, and A. Tani, “FOC and DTC: Two viable schemes for induction motors torque control,” IEEE Trans. on Power Electron., vol. 17, no. 5, pp. 779–787, Sep. 2002.
3. K. K. Mohapatra, R. S. Kanchan, M. R. Baiju, P. N. Tekani, and K. Gopakumar, “Independent field-oriented control of two split-phase induction motors from a single six-phase inverter,” IEEE Trans. Ind. Electron., vol. 52, no. 5, pp. 1372–1382, Oct. 2005.
4. A. Jidin, N. R. N. Idris, A. H. M. Yatim, T. Sutikno, and M. E. Elbuluk, “An Optimized Switching Strategy for Quick Dynamic Torque Control in DTC-Hysteresis-Based Induction Machines,” IEEE Trans. Ind. Electron., vol. 58, no. 8, pp. 3391–3400, Aug. 2011.
5. Y. Zhang, J. Zhu, Z. Zhao, W. Xu, and D. G. Dorrel, “An improved direct torque control for three-level inverter-fed induction motor sensorless drive,” IEEE Trans. Power Electron., vol. 27, no. 3, pp. 1502–1513, Mar. 2012.
6. Y. S. Choi, H. H. Choi, and J. W. Jung, “Feedback linearization direct torque control with reduced torque and flux ripples for IPMSM drives,” IEEE Trans. Power Electron., vol. 31, no. 5, pp. 3728–3737, May 2016.
7. M. Deepu, X. Zhang, and G. H. B. Foo, “Three-level inverter-fed direct torque control of IPMSM with constant switching frequency and torque ripple reduction,” IEEE Trans. Ind. Electron., vol. 63, no. 12, pp. 7908–7918, Dec. 2016.
8. J. K. Pandit, M. V. Aware, R. V. Nemade, and E. Levi, “Direct Torque Control scheme for a six-phase induction motor with redued torque ripple,” IEEE Trans. Power Electron., vol. 32, no. 9, pp. 7118–7129, Sep. 2017
9. Y. N. Tatte and M. V. Aware, “Torque ripple and Harmonic current reduction in a Three-level inverter-fed direct torque controlled Five-phase induction motor,” IEEE Trans. Ind. Electron., vol. 64, no.7,pp. 5265–5275, Jul. 2017.
10. Y. N. Tatte and M. V. Aware, “Direct Torque Control of five-phase induction motor with common-mode voltage an current harmonics reduction,” IEEE Trans. Power Electron., vol. 32, no.11, pp. 8644–8654, Nov. 2017.

Published By:
Blue Eyes Intelligence Engineering and Sciences Publication (BEIESP)

11. G. S. Buja and M. P. Kazmierkowski, "Direct torque control of PWM inverter-fed AC motors- A survey," IEEE Trans. Ind. Electron., vol. 51, no. 4,pp. 744–757, Aug. 2004.
12. D. Casadei, G. Serra, A. Tani, and L. Zarri, "Direct torque control for induction machine: a technology status review,"in Proc. Int. Conf. WEMDCD,Delhi, india, Jan. 2013, pp. 117–129.
13. F. Niu, B. Wang, A. S. Babel, K. Li, and E. G. Strangas, "Comparative evaluation of Direct Torque Control strategies for Permanent Magnet Synchronous Machines," IEEE Trans. Power Electron., vol. 31, no. 2, pp. 1408–1424, Feb. 2016.
14. J. Rodriguez, J.-S. Lai, and F. Z. Peng, "Multilevel Inverters: A Survey of Topologies, Controls, and Applications," IEEE Trans. Ind. Electron., vol. 49, no. 4, pp. 724–736, Aug. 2002
15. S. Kouro, R. Bernal,H. Miranda, C. A. Silva, and J. Rodriguez, "High performance torque and flux control for multilevel inverter fed induction motors," IEEE Trans. Power Electron., vol. 22, no. 6, pp. 2116–2123, Nov. 2007.
16. F. Khoucha, S. M. Lagoun, K. Marouani, A. Kheloui, and M. E. H. Benbouzid, "Hybrid cascaded H-Bridge multilevel-inverter induction-motor-drive direct torque control for automotive applications," IEEE Trans. Ind. Electron., vol. 57, no. 3,pp. 892–899, Mar. 2010.
17. V. T. Somasekhar, K. Gopakumar, M. R. Baiju, K. K. Mohapatra, and L. Umanand, "A multilevel inverter system for an induction motor with open-end winding," IEEE Trans. Ind. Electron., vol. 52, no. 3, pp. 824–836, Jun. 2005.
18. M. R. Baiju, K. Gopakumar, K. K. Mohapatra, V. T. Somasekhar, and L. Umanand, "Five-level inverter voltage-space phasor generation for an open-end winding induction motor drive," IEE Proc.-Electr. Power Appl., vol. 150, no. 5, pp. 531–538, Sep 2003.
19. C. Patel, P. P. Rajeevan,A. Dey, R. Ramchand, K. Gopakumar, and M. P. Kazmierkowski, "Fast direct torque control of an open-end induction motor drive using 12-sided polygonal voltage space vectors," IEEE Trans. Power Electron., vol. 27**,** no. 1,pp. 400–410, Jan. 2012.
20. M. K. Rahim, F. Patkar,A. Jidin, and A. Razi, "Reduced torque ripple and switching frequency using optimal dtc switching strategy for open-end winding of induction machines," in Proc. IEEE Int. Conf. PEDS, Jun. 2015, pp. 767-772.
21. N. Celanovic and D. Boroyevich, "A fast space vector modulation algorithm for multilevel three-phase converters,"IEEE Trans. Ind. Appl., vol. 37, no. 2, pp. 637–641, Apr. 2001.
22. A. Gopinath, A. S. Aneesh Mohamed, and M. R. Baiju, "Fractal based space vector PWM for inverters – A novel approach," IEEE Trans. Ind. Electron., vol. 52, no. 4, pp. 1230–1238, Apr. 2009.
23. Shiny G. and M. R. Baiju, "Fractal based low computation space phasor generation scheme for a four-level inverter using an open-end winding induction motor," IET Electr. Power Appl., vol. 6, no. 9, pp. 652–660, Jun. 2012.
24. Shiny G. and M. R. Baiju, "Space vector pulse width modulation strategy for an even level inverter," in IEEE Int. Conf. TAP ENERGY 2017, to be published.
25. B. Jacob and M. R. Baiju, "Space-vector quantized dithered sigma-delta modulator for reducing the harmonic noise in multilevel converters," IEEE Trans. Ind. Electron., vol. 62, no. 4, pp. 2064–2072, Apr. 2015.
26. Joohn-Sheok Kim and Seung-Ki Sul, "A Novel Voltage Modulation Technique of the Space Vector PWM," in Proc. Int. Conf. IPEC Yokohama, 1995, pp. 742–747.
27. Z. Zhang, Y. Zhao, W. Qiao, and L. Qu, "A Space Vector Modulated Sensorless Direct Torque control for Direct-Drive PMSG Wind Turbines," IEEE Trans. Ind. Appl., vol. 50, no. 4, pp. 2331–2341, Aug. 2014.
28. N. Venkataramana Naik, A. Panda, and S. P. Singh, "A three-level Fuzzy-2 DTC of induction motor drive using SVPWM," IEEE Trans. Ind. Electron., vol. 63, no. 3, pp. 1467–1479, Mar. 2016.
29. A. H. Abosh, Z. Q. Zhu, and Y. Ren, "Reduction of torque an flux ripples in Space Vector Modulation-based Direct Torque Control of asmmetric Permanent Magnet Synchronous Machine," IEEE Trans. Power Electron., vol. 32, no. 4, pp. 2976–2986, Apr. 2017.
30. Vinod B. R., M. R. Baiju, and Shiny G., "Five level inverter fed space vector based direct torue control of open-end winding induction motor drive," IEEE Trans. Energy Convers., Mar. 2018, accepted for publication.

AUTHOR PROFILE

Vinod B. R. received the B. E. Degree in Electronics and Communication Engineering from Bharathiar University, India, in 1993, and the M. E. Degree in Control System from Anna University, Chennai, India, in 2008.

From 1999 to 2004, he was with the Kerala State Electricity Board, India. Since 2004, he has been a faculty member with the Department of Electronics and Communication Engineering, College of Engineering Trivandrum, Kerala, India. He is currently working toward the Ph.D. Degree at University of Kerala, India. His research interests include space vector based direct torque control drives and multilevel inverter fed induction motor drives.

Shiny G. received the B. E. Degree in Electronics and Communication Engineering from Madurai Kamaraj University, India, in 1990, and the M.Tech and Ph.D Degrees from University of Kerala, India, in 1994 and 2013, respectively.

Since 1998, she is with Technical Education Department, Govt. of Kerala, India. Since 2005, she has been a faculty member with the Department of Electronics and Communication Engineering, College of Engineering Trivandrum, Kerala, India. Her research interest includes multilevel inverter topologies, inverter control strategies, FPGA baesd PWM switching schemes for multilevel inverters, and vector controlled drives.

Published By:
Blue Eyes Intelligence Engineering and Sciences Publication (BEIESP)